LA-UR-92-4376
N-6-92-R220

In Proceeding "Fourth Int. Conf. of High Level Rad. Waste Manage." April 26-30, Las Vegas, NV, USA.

TITLE: APERTURE CHARACTERISTICS, SATURATED FLUID FLOW, AND TRACER TRANSPORT CALCULATIONS FOR A NATURAL FRACTURE

AUTHOR(S): P. W. Reimus
B. A. Robinson
R. J. Glass

SUBMITTED TO: 1993 International High-Level Radioactive Waste Management Conference
April 26-30, 1993
Las Vegas, Nevada

Los Alamos National Laboratory
Los Alamos, New Mexico 87545

APERTURE CHARACTERISTICS, SATURATED FLUID-FLOW, AND TRACER-TRANSPORT CALCULATIONS FOR A NATURAL FRACTURE

P. W. Reimus and B. A. Robinson
Los Alamos National Laboratory
P.O. Box 1663
Los Alamos, NM 87545
(505) 665-2537 and (505) 667-1910

R. J. Glass
Sandia National Laboratories
P.O. Box 5800
Albuquerque, NM 87185
(505) 844-4809

ABSTRACT

We used surface-profile data taken with a noncontact laser profilometer to determine the aperture distribution within a natural fracture and found the surfaces and apertures to be isotropic. The aperture distribution could be described equally well by either a normal or a lognormal distribution, although we had to adjust the standard deviation to "fit" the data. The aperture spatial correlation varied over different areas of the fracture, with some areas being much more correlated than others. The fracture surfaces did not have a single fractal dimension over all length scales, which implied that they were not self-similar.

We approximated the saturated flow field in the fracture by solving a finite-difference discretization of the fluid-flow continuity equation in two dimensions. We then calculated tracer breakthrough curves using a particle-tracking method. Comparing the breakthrough curves obtained using both coarse- and fine-resolution aperture data (0.5- and 0.05-mm spacing between points, respectively) over the same subset of the fracture domain suggests that the spacing between the aperture data points must be less than the correlation length to obtain accurate predictions of fluid flow and tracer transport. In the future, we will perform tracer experiments and numerical modeling studies to determine exactly how fine the aperture data resolution must be (relative to the correlation length) to obtain accurate predictions.

INTRODUCTION

Fluid flow and tracer transport in saturated natural fractures have been studied extensively in the past 10–15 yr. The studies have been motivated largely by the need to better understand contaminant transport in fracture systems. A good review of fracture flow and transport studies through 1990 is provided by Wang.[1]

The overall objective of this study is to conduct tracer-transport experiments in natural fractures with sufficiently well characterized flow fields that the effects of flow-field dispersion on observed transport behavior can be separated from the effects of tracer interactions with rock surfaces (adsorption and matrix diffusion). Two questions must be addressed before such a goal can realistically be met.

1. What spatial resolution and precision of fracture aperture data are necessary (relative to the aperture correlation length) to obtain accurate flow-field predictions?

2. What practical limitations exist in modeling tracer-transport experiments or, conversely, in designing experiments to satisfy model assumptions?

In this paper, we describe progress that has been made to address these questions.

Our principal accomplishments to date have been to

1. obtain aperture data in a natural fracture at different spatial resolutions using surface profile data taken with a noncontact laser profilometer,

2. determine the statistical and fractal characteristics of the surfaces and apertures based on these data,

3. determine the best set of experimental conditions under which to run fluid-flow and tracer-transport experiments in natural fractures, and

4. perform calculations of fluid flow and tracer transport in fractures using the experimental aperture data.

Our method of obtaining the aperture data is different from that used by others,[2-5] and it ultimately will be compared with at least one of these other methods. The fluid-flow and tracer-transport calculations have provided us with some initial insight into the question of how fine the spatial resolution of the aperture data must be to obtain accurate flow-field predictions. This issue will be the focus of future work.

FRACTURE SPECIMEN AND SURFACE TOPOGRAPHY MEASUREMENTS

A natural fracture was taken from an outcropping of Bandelier tuff in the Jemez Mountains about 4 miles west of Los Alamos, New Mexico. The rock was cut into a rectangular block approximately 11.6 x 10.4 x 5.3 cm using a diamond-tipped rock saw; the fracture bisected the 5.3-cm dimension. (The fracture surface area was 11.6 x 10.4 cm^2). Profiles of the fracture surfaces were obtained using a noncontact laser profilometer similar to the one described by Huang et al.[6] The laser beam has a cross-sectional area of approximately 0.0254 x 0.0254 mm^2, and the vertical precision of the instrument is about 0.007 mm, which is the standard deviation of repeated measurements taken at a fixed point on an opaque surface. Three different sets of profiles were obtained on each surface.

1. Linear profiles: Two groups of five linear profiles, each 97.968 mm long with 0.0254-mm spacing between points (the width of laser beam), were taken in the direction of the 10.4-cm dimension of the fracture surface. The spacing between profiles within each group was 0.05 mm.

2. Coarse-resolution two-dimensional profile: A two-dimensional profile over a 110.0- x 98.0-mm^2 area was taken with 0.5-mm spacing between points.

3. Fine-resolution two-dimensional profile: A two-dimensional profile over a 9.95- x 9.95-mm^2 area was taken with 0.05-mm spacing between points.

In all three cases, the profiles on each surface were intended to "match" when the two surfaces were mated.

SURFACE AND APERTURE CHARACTERISTICS

The raw surface profile data were manipulated as follows to obtain aperture data.

1. The data from one of the surfaces were "flipped" to match the data on the other surface. (The two surfaces were profiled as mirror images of each other.)

2. A plane was fit to the data from each surface by multiple linear regression (a line was fit to the linear profile data). This plane then was subtracted from the data so that the data became distributed about a plane of zero height.

3. All the data from one of the surfaces were multiplied by -1 so that a peak on one surface would correspond to a valley on the other surface.

4. The adjusted data were "matched" by moving one data set relative to the other until the minimum mean square error between the two surfaces was obtained.

5. The surfaces were separated until they touched at only one point. The local apertures were calculated from the separation between each matched pair of data points.

6. As a final refinement, a plane was fit to the aperture data by multiple linear regression, and the linear components of the plane (not the constant) were subtracted from the data. This adjustment removed any unrealistic trend from the data that may have resulted from the inclusion of nonmatching points when the plane was fit to the surface data.

The apertures obtained with this procedure were unrealistically large (a mean of 0.61809 mm for the coarse-resolution two-dimensional aperture data) because there were a few anomalous surface elevations that resulted either from instrument error or from foreign debris on the surfaces during profiling. The frequency distribution of the coarse-resolution aperture data is shown in Figure 1 along with normal and lognormal distributions that were generated using the mean of the data and a standard deviation that was adjusted to "fit" the data. When the actual standard deviation of the data (0.06887 mm) was

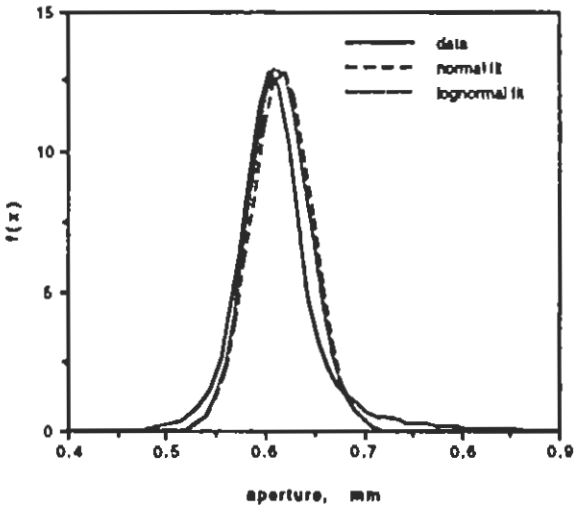

Figure 1 - Frequency distribution of the coarse-resolution aperture data (0.5-mm spacing between points over an 11.0- x 9.65-cm^2 area). The data have a mean = 0.61809 mm and a standard deviation = 0.06887 mm; the normal distribution has a mean = 0.61809 and a standard deviation = 0.031 mm; and the lognormal distribution has a mean of log data = -0.486 and a standard deviation of log data = 0.05.

used, the mathematically generated distributions were much too broad to fit the data. Apparently, the standard deviation of the data was biased by a few very large and very small apertures. Even if these outlier apertures were real, it is unlikely that they would affect fluid-flow or tracer-transport calculations significantly unless they were highly correlated, which was not the case for this data set. Because of the low frequency and lack of correlation of the very large and small apertures, we believe that it is better to characterize the distribution using a standard deviation adjusted to fit the majority of the data rather than to use the actual standard deviation. From Figure 1, it is apparent that the normal and lognormal distributions with adjusted standard deviations fit the data about equally well.

The spatial correlations of the apertures in various directions in the fracture plane were determined by plotting the directional autocorrelation functions vs lag. The autocorrelation function is defined as

$$r_k = \frac{1}{\sigma^2(n-k-1)} \sum_{i=1}^{n-k} (x_{i+k} - \mu)(x_i - \mu) \ , \qquad (1)$$

where x_i = the value associated with data point i, μ = the mean of the data, σ^2 = the variance of the data, n = the number of data points, and k = the lag (in number of data points). For the two-dimensional aperture data, the autocorrelation was determined in the horizontal, vertical, and diagonal directions. A plot of the autocorrelation vs lag for the fine-resolution two-dimensional aperture data (0.05-mm spacing between points) is shown in Figure 2.

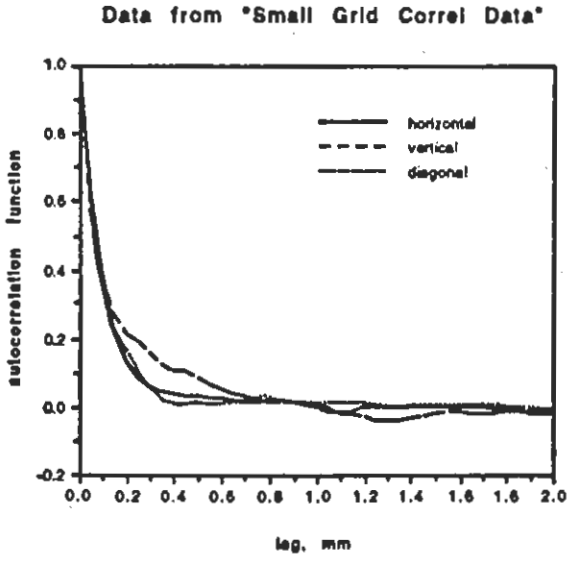

Figure 2 - Aperture autocorrelation function vs lag for the fine-resolution aperture data (0.05-mm spacing between points over a 0.965- x 0.635-cm^2 area) in the horizontal, vertical, and diagonal directions in the fracture plane.

For each set of data and each direction, the autocorrelation appeared to decay approximately exponentially with lag, so we estimated a correlation length, L, by assuming an autocorrelation function of the form $r_k = \exp(-k/L)$ and using regression to obtain an estimate of L. The estimates of the directional correlation lengths from the different sets of aperture data are given in Table I. It

Table I - Directional correlation lengths estimated from the different aperture data sets.

Spacing Between Points (Direction)	Correlation Length (mm)
0.0254 mm (horizontal)	0.231
0.05 mm (horizontal, diagonal)	0.232
0.05 mm (vertical)	0.229
0.5 mm (all three directions)	1.450

is apparent that the aperture distribution is reasonably isotropic, but it is interesting that the correlation length obtained from the coarse-resolution aperture data is about a factor of 6 larger than that obtained from the fine-resolution data. There are at least two possible explanations for this difference: (1) the small region of the fracture that was profiled at the fine resolution had an abnormally small spatial correlation relative to the rest of the fracture and/or (2) there is a "scale effect" when correlation lengths are determined from data having different resolutions in the fracture plane. Although we cannot rule out the latter possibility until further analysis is done, we believe that the former explanation is valid because a subset of the coarse-resolution aperture data corresponding to the area over which the fine-resolution data were obtained was found to be essentially uncorrelated. This result is not surprising because the correlation length over this region was about 0.23 mm and the spacing between the coarse-resolution data points was 0.5 mm.

The surface and aperture distributions also were characterized using spectral methods. We used the procedure of Brown and Scholz[7] to obtain the Fourier transform power spectra of the surface and aperture data in various directions within the fracture plane. The ensemble surface and aperture power spectra associated with the linear profiles are shown in Figure 3. The roll-off in the aperture power spectrum at small frequencies (large wavelengths) occurs because the apertures have a well-defined maximum, which tends to limit the amplitudes of the sine and cosine components of the Fourier transform at large wavelengths. The surface spectrum does not exhibit this roll-off because the amplitudes of surface features tend to keep increasing with wavelength. These and other properties of surface and aperture power spectra are discussed in more detail elsewhere.[7,8] The noise line in Figure 3 is a power spectrum for a string of random numbers with a mean of zero and a standard deviation of 0.01 mm, which

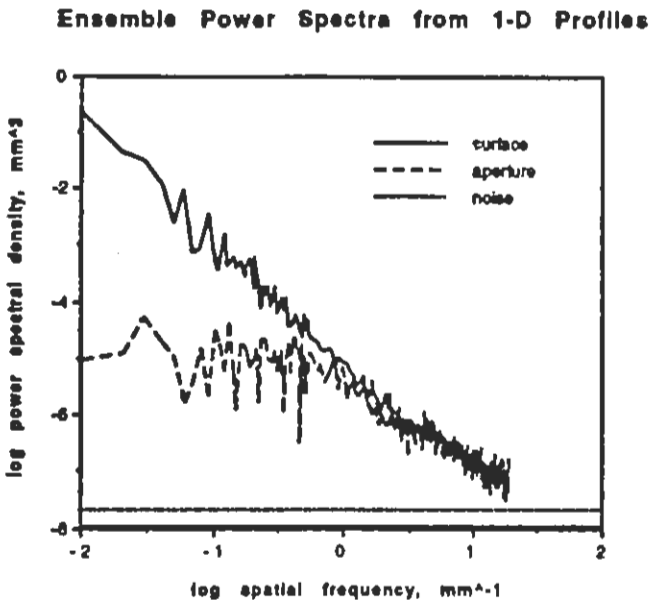

Figure 3 - Ensemble surface and aperture power spectra associated with the linear surface profiles with 0.0254-mm spacing between data points.

is approximately the standard deviation of the laser profilometer. If the surface and aperture power spectra were to be extended to higher frequencies, they would level off and follow the noise spectrum because the profile measurements would be limited by the precision of the profilometer.

As discussed by Brown and Scholz[7] and Wang et al.,[9] the fractal dimension of a fracture surface is proportional to the slope of its power spectrum. If the power spectrum is linear over all wavelengths, then the surface is characterized by a single fractal dimension, and it is said to be "self-similar." Surface anisotropy is indicated by differences in the slope or intercept of power spectra corresponding to different directions on the surface. In this study, the ensemble surface power spectra were consistently nonlinear, with a greater negative slope at lower frequencies than at higher frequencies. This trend is in contrast to that observed by Brown and Scholz,[7] who noted a greater negative slope as frequency increased for 8 out of 10 rock specimens. The apparent fractal dimension of the Bandelier tuff surfaces ranged from about 2.4 at low frequencies to 2.8 at higher frequencies. (2.0 corresponds to a perfectly flat surface, and 3.0 corresponds to a very rough surface.) Brown and Scholz[7] and Brown et al.[8] report fractal dimensions ranging from 2.0 to 2.7 for several natural fracture surfaces. The surface and aperture power spectra in different directions in the fracture plane were nearly identical, indicating that the Bandelier tuff fracture was reasonably isotropic.

HYDRAULIC APERTURE EXPERIMENTS

A flow apparatus was built around the Bandelier tuff fracture by sandwiching the fracture between two 1/2-in.-thick aluminum plates held together by bolts at the corners. The normal pressure holding the fracture together could be adjusted crudely by tightening the bolts to different torques using a torque wrench. The sides of the fracture were sealed to yield no-flow boundaries using the method illustrated in Figure 4. The inlet and outlet ends of the fracture were sealed in the same way, except that an open area was cut into the gasket material to allow a fluid to be introduced to the fracture through holes cut into the aluminum plates placed over the gasket material.

Hydraulic aperture experiments were conducted by applying a constant head across the fracture and measuring the fracture flow rate by collecting and weighing the water flowing through the fracture over a given period of time. The hydraulic aperture is defined by

$$b_{byd} = \left(\frac{12\mu QL}{\rho g W \Delta H}\right)^{1/3}, \qquad (2)$$

where Q = the volumetric flow rate through fracture, L = the length of fracture, W = the width of fracture, ρ = the fluid density, g = the gravity acceleration, and ΔH = the head difference across fracture. Physically, it is the distance that parallel plates of the same length and width as the natural fracture would have to be separated by to have the same flow rate vs. pressure drop dependence as the natural fracture. We conducted a number of experiments to determine the sensitivity of the hydraulic aperture to different experimental conditions and to try to identify the optimal conditions under which tracer-transport experiments should be run. Our main findings are listed below.

1. The hydraulic aperture was very sensitive to the normal pressure holding the fracture together; the hydraulic aperture decreased

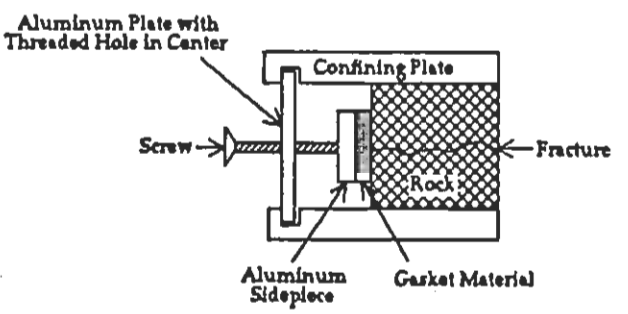

Figure 4 - Side view of sealing method for no-flow boundaries of fracture flow apparatus.

dramatically with increases in normal pressure. It was very difficult to reproduce the hydraulic aperture in consecutive experiments. Part of the problem may have been that a nonreproducible tangential shearing stress was exerted on the fracture surfaces when the sides and ends of the fracture were sealed. The hydraulic aperture varied from 0.0243 to 0.0489 mm despite attempts to keep it approximately the same in each test. The reproducibility seemed to be better when the normal pressure holding the fracture was increased, probably because of the increasing stiffness of the joint at higher normal pressures.

2. When deionized water was used, the hydraulic aperture gradually decreased with time, and the fracture eventually became sealed such that the flow rate through the fracture could no longer be measured. Through experimental control, we ruled out biological growth, swelling of rock minerals, and filtration of particulates in the water as possible explanations for this phenomenon. We believe that the sealing process may have been the result of dissolution reactions occurring at the fracture walls. These dissolution reactions could have either (1) caused relatively large grains to break free from the walls and move downstream until they became trapped in narrow constrictions where they became obstacles to flow or (2) preferentially occurred at stressed contact points within the fracture, thereby causing the mean fracture aperture to decrease with time. We will test the dissolution hypothesis in the future by using water that is chemically equilibrated with the rock in the flow experiments, which should significantly reduce the driving force for dissolution. We also will check the fracture effluent for particles to test the grain spallation hypothesis.

3. The hydraulic aperture was somewhat sensitive to the pressure drop across the fracture; the aperture increased as the pressure drop increased. Because the head on the outlet side of the fracture was always the same, we suspect that the fracture widened primarily at the upstream end of the fracture. This widening effect was less pronounced when the normal pressure holding the fracture together was increased.

4. The best results were obtained when the fracture specimen was saturated with water under vacuum before assembling the flow apparatus and when the surfaces were mated under water to avoid the introduction of air into the fracture during assembly.

Based on these conclusions, it will be best to use a relatively high normal pressure to hold the fracture surfaces together and to use water that is equilibrated with the rock in future tracer-transport experiments.

FLOW-FIELD CALCULATIONS

Flow fields associated with the two-dimensional aperture distributions deduced from the surface profile data were calculated using a finite-difference discretization of the fluid-flow continuity equation derived by assuming that parabolic flow occurs within each cell.[10-16] The continuity equation (assuming square cells) is

$$\frac{\partial}{\partial x}\left[b^3(x,z)\frac{\partial p(x,z)}{\partial x}\right]+\frac{\partial}{\partial z}\left[b^3(x,z)\frac{\partial p(x,z)}{\partial z}\right]=0 \ , \quad (3)$$

where p = the pressure and b(x,z) = the local aperture. Boundary conditions consistent with those in the hydraulic aperture experiments were imposed (constant pressure at ends, no flow through sides). We solved the discretized form of Equation (3) by matrix inversion using an iterative sparse matrix solver developed at Los Alamos National Laboratory.[17] After solving for the pressure distribution, we obtained the flow rate between adjacent cells from

$$Q = W\left(\frac{b_{eff}^3}{12\mu}\right)\frac{(p_1-p_2)}{(x_1-x_2)} \ , \quad (4)$$

where Q = the volumetric flow rate across boundary, W = the width of boundary, μ = the fluid viscosity, p_i = the pressure in cell i, x_i = the coordinate of center of cell i in direction of flow, and

$$b_{eff} = \left[\frac{2b_1^3 b_2^3}{b_1^3+b_2^3}\right]^{1/3} .$$

The flow rates across each of the four boundaries of a cell were added vectorially to obtain a single velocity vector for each cell.

The coarse-resolution aperture data were adjusted until the calculated hydraulic aperture fell within the range of hydraulic apertures measured in the experiments. The adjustment was made by subtracting a constant from all apertures and setting any negative apertures equal to zero. The mean aperture had to be reduced from 0.6181 to 0.0559 mm to obtain a hydraulic aperture of 0.0386 mm, which was approximately halfway between the largest and smallest experimental hydraulic apertures. This reduction in the mean aperture resulted in an 8.5% contact area between the two surfaces, which is not unreasonable when compared with the experimental contact areas reported by Pyrak-Nolte et al.[2] (8 to 15%) or the contact areas reported by Brown[10] and Thompson[16] when mathematically generated surfaces having a fractal dimension of 2.5 were brought together until their separation relative to the aperture standard deviation was about the same as for our

surfaces. When our mean aperture was adjusted to 0.0689 mm and 0.1377 mm (one and two standard deviations), the hydraulic aperture was 0.055 mm and 0.126 mm, respectively. These ratios of hydraulic aperture to mean aperture are in good agreement with the results of Brown[10] and Thompson[16] for mathematically generated fractal surfaces at the same relative surface separations.

The flow field associated with the coarse-resolution aperture data after the mean aperture was adjusted to 0.0559 mm is shown in Figure 5. The lengths of the vectors are proportional to the local volumetric flow rates. Only every third vector in each direction is plotted to avoid excessive clutter. The calculation was done for a finite-difference grid of 221 x 194 cells. It is apparent from Figure 5 that although some flow channeling in the fracture is predicted, there are no dominant flow channels. Significant channeling does not occur because the average correlation length of the apertures in any direction is only about three cell lengths or about 1.5% of the overall dimensions of the flow domain. In studies where aperture distributions are generated mathematically for flow-field calculations, the correlation length is typically at least 10% of the flow domain dimensions, with the result being that there are well-defined flow channels.[10-14,16]

TRACER-TRANSPORT CALCULATIONS

Tracer breakthrough curves associated with the calculated flow fields were predicted using a particle tracking method similar to that described by others.[11,14,18,19] Our calculations generated a tracer breakthrough curve in response to a step function input from the cumulative residence time distribution of 10,000 particles that moved through the fracture. Monte Carlo methods were used to make decisions about the pathways taken by the particles. The probabilities of entering a given discretized cell were proportional to the flow rate into that cell. Tracer travel times were obtained by summing the particle residence times in each cell, which were assumed to be inversely proportional to the average flow velocity in each cell. Breakthrough curves were calculated for the coarse-resolution aperture data, the fine-resolution aperture data, and a subset of the coarse-resolution aperture data corresponding to the same area of the fracture as the fine-resolution aperture data (0.995 x 0.635 cm^2). In all cases, the mean tracer residence time was within about 2% of the mean fluid residence time, which is expected for particle tracking calculations.[18,19]

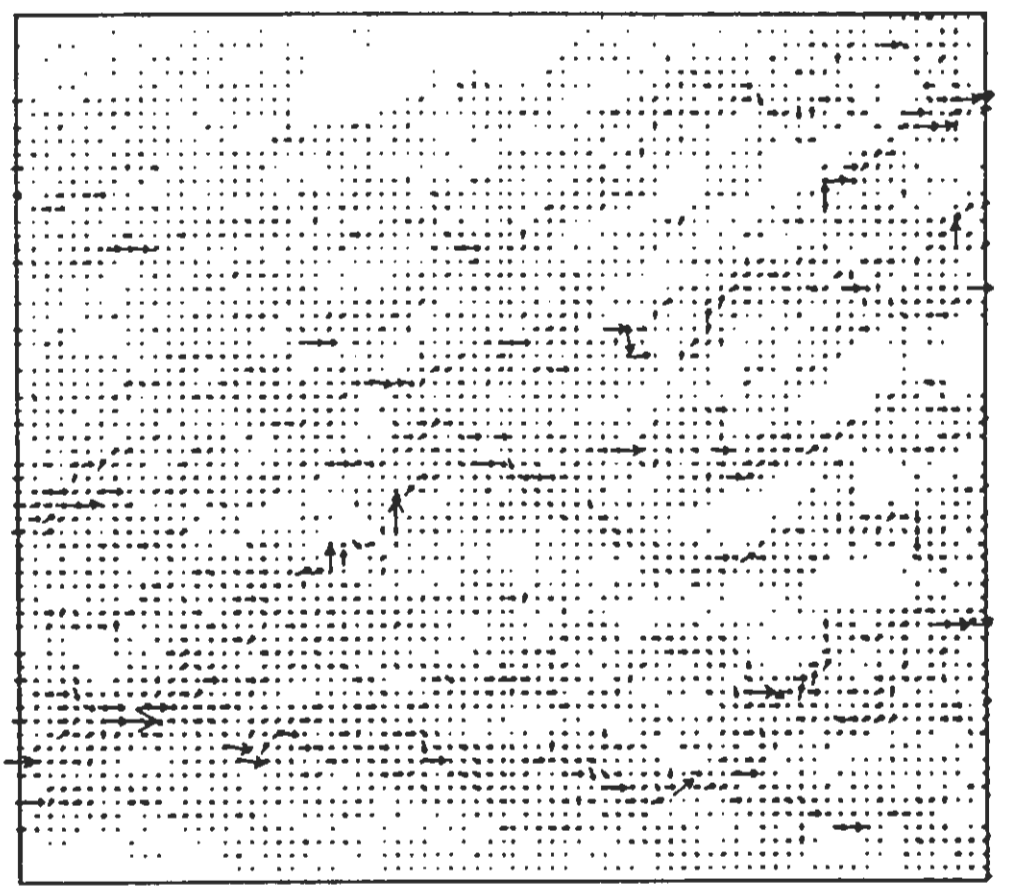

Figure 5 - Flow field associated with the adjusted coarse-resolution aperture data (0.5-mm spacing between points over an 11.0- x 9.65-cm^2 area). The mean aperture was 0.0559 mm, and the hydraulic aperture was calculated to be 0.0386 mm.

In the absence of any experimental data, the breakthrough curves of greatest interest are the ones associated with the coarse- and fine-resolution aperture data over the 0.995- x 0.635-cm^2 area. A comparison of these breakthrough curves offers insights into how sensitive the tracer-transport predictions are to the resolution of the aperture data, and in particular, whether aperture data that have a spacing between points greater than the correlation length is of any value in predicting flow and tracer transport in fractures. Representative breakthrough curves associated with the two sets of aperture data are shown in Figure 6. Both curves were calculated with the assumptions that there was no matrix diffusion and there were no tracer interactions with fracture walls. The two aperture data sets were adjusted so that their mean surface separation was the same, which resulted in a slight difference in the hydraulic apertures (0.0495 mm for the coarse data and 0.0519 mm for the fine data). As noted earlier, the coarse-resolution aperture data were essentially uncorrelated, and the fine-resolution data had a correlation length equal to about five cell lengths. From Figure 6, it is apparent that the breakthrough curve associated with the fine-resolution data is not reproduced when the coarse-resolution data are used, which leads to the conclusion that uncorrelated aperture data are probably of little value when trying to predict tracer transport. However, a key question remains—can the coarse-resolution aperture data over 88.5% of the fracture area, which had an average correlation length of about three cell lengths, provide accurate predictions of tracer transport in the fracture? This question will be addressed by conducting tracer experiments in the fracture and comparing the experimental breakthrough curves with predicted breakthrough curves.

FUTURE WORK

Besides conducting tracer experiments in the Bandelier tuff fracture, we will perform the following activities to further address the objectives of this study.

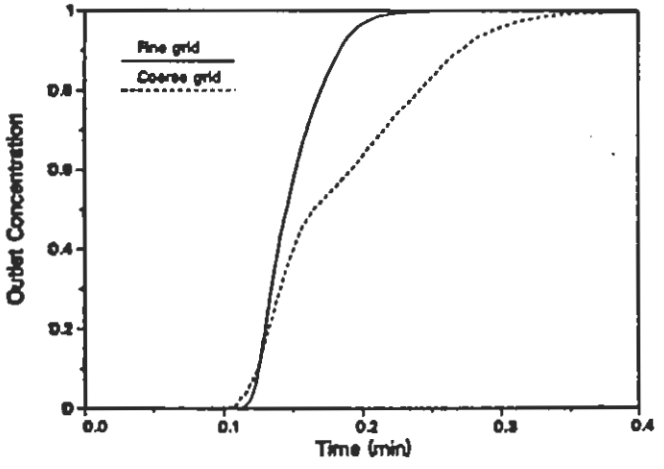

Figure 6 - Tracer breakthrough curves calculated from the coarse- and fine-resolution aperture data over the 0.965- x 0.635-cm^2 area. Differential head was 0.0167 ft H_2O.

1. A numerical modeling study will be conducted in which a mathematically generated aperture distribution is "coarsened" systematically so that fluid-flow and tracer-transport calculations are based on aperture data that are progressively less correlated. It is hoped that a practical limit can be determined for the resolution of aperture data (relative to the correlation length) that are necessary to provide accurate predictions of tracer transport in fractures. This study also could be done using real aperture data if the resolution of the data is fine relative to the correlation length.

2. An RTV silicone rubber cast of the void space in the Bandelier tuff fracture will be made, and the fracture aperture distribution will be determined by measuring light transmittance as a function of position through the cast.[4,5] This technique will provide an independent verification of the aperture distribution deduced from the laser profilometer data, and it may offer advantages over the surface profiling technique.

3. An epoxy replica of the Bandelier tuff fracture will be made using the methods of Hakami and Barton[3] and Persoff et al.[20] Tracer-transport experiments will then be performed in the epoxy fracture. The epoxy replica will offer at least three experimental advantages over the natural fracture: (1) matrix diffusion will be eliminated, (2) the surfaces will be chemically homogeneous, and (3) it should be possible to observe tracer movement through the fracture in real time. These features will help in the interpretation of the experiments, and they will simplify the tracer-transport modeling. The aperture distribution in the epoxy replica also will be measured so that the apertures in the real fracture and the replica can be compared to determine how precise the replication is.

4. An attempt will be made to determine the void volume of the fracture under experimental conditions using either a fluid injection technique (for example, measuring weight difference as solution is injected into the fracture or as solution density is changed), a Woods metal technique,[2] a tracer technique,[19] or possibly the method of Hakami and Barton,[3] which involves placing a known volume of liquid in the void space of an epoxy replica and then measuring the area occupied by the liquid after mating the surfaces (this provides an estimate of the void volume over a subset of the fracture area). An estimate of the void volume will allow a determination of whether the aperture adjustment necessary to match the experimental hydraulic aperture results in a realistic surface separation.

ACKNOWLEDGMENTS

This work was supported by the Yucca Mountain Project Site Characterization Project Office as part of the Civilian Radioactive Waste Management Program. This Project is managed by the U.S. Department of Energy, Yucca Mountain Site Characterization Project. Stephen Brown and Robert Hardy of Sandia National Laboratories provided the surface profile data from the noncontact laser profilometer.

DISCLAIMER

In accordance with Administrative Procedure 5.1Q, this paper contains no new scientific or engineering data. The computer calculations presented in this paper were performed using software not developed in accordance with a Software Quality Assurance Plan.

REFERENCES

1. J. S. Y. WANG, "Flow and Transport in Fractured Rocks," Rev. Geophys., Suppl., U.S. National Report to International Union of Geodesy and Geophysics 1987-1990, pp. 254-262 (1991).

2. L. J. PYRAK-NOLTE, L. R. MYER, N. G. W. COOK, and P. A. WITHERSPOON, "Hydraulics and Mechanical Properties of Natural Fractures in Low Permeability Rocks," Sixth International Congress on Rock Mechanics, Int. Soc. for Rock Mech., Montreal, Canada (1987).

3. E. HAKAMI and N. BARTON, "Aperture Measurements and Flow Experiments Using Transparent Replicas of Rock Joints," Rock Joints, Barton and Stephansson, eds., Balkema, Rotterdam, pp. 383-390 (1990).

4. S. GENTIER, D. BILLAUX, and L. VAN VLIET, "Laboratory Testing of the Voids of a Fracture," Rock Mech. and Rock Eng., 22, 149 (1989).

5. B. L. COX, K. PRUESS, and P. PERSOFF, "A Casting and Imaging Technique for Determining Void Geometry and Relative Permeability Behavior of a Single Fracture Specimen," LBL-28485, Lawrence Berkeley Laboratory (1990).

6. C. HUANG, I. WHITE, E. G. THWAITE, and A. BENDELI, "A Noncontact Laser System for Measuring Soil Surface Topography," Soil Sci. Am. J., 52, 350 (1988).

7. S. R. BROWN and C. R. SCHOLZ, "Broad Bandwidth Study of the Topography of Natural Rock Surfaces," J. Geophys. Res., 90(B14), 12575 (1985).

8. S. R. BROWN, R. L. KRANZ, and B. P. BONNER, "Correlation Between the Surfaces of Natural Rock Joints," Geophys. Res. Let., 13(13), 1430 (1986).

9. J. S. Y. WANG, T. N. NARASIMHAN, and C. R. SCHOLZ, "Aperture Correlation of a Fractal Fracture," J. Geophys. Res., 93(B3), 2216 (1988).

10. S. R. BROWN, "Fluid Flow Through Rock Joints: The Effect of Surface Roughness," J. Geophys. Res., 92(B2), 1337 (1987).

11. L. MORENO, Y. W. TSANG, C. F. TSANG, F. V. HALE, and I. NERETNIEKS, "Flow and Tracer Transport in a Single Fracture: A Stochastic Model and Its Relation to Some Field Observations," Water Resour. Res., 24(12), 2033 (1988).

12. S. R. BROWN, "Transport of Fluid and Electrical Current Through a Single Fracture," J. Geophys. Res., 94(B7), 9429 (1989).

13. Y. W. TSANG and C. F. TSANG, "Flow Channeling in a Single Fracture as a Two-Dimensional Strongly Heterogeneous Permeable Medium," Water Resour. Res., 25(9), 2076 (1989).

14. L. MORENO, C. F. TSANG, Y. TSANG, and I. NERETNIEKS, "Some Anomalous Features of Flow and Solute Transport Arising from Fracture Aperture Variability," Water Resour. Res., 26(10), 2377 (1990).

15. R. G. STRATFORD, A. W. HERBERT, and C. P. JACKSON, "A Parameter Study of the Influence of Aperture Variation on Fracture Flow and the Consequences in a Fracture Network," Rock Joints, Barton and Stephansson, eds., Balkema, Rotterdam, pp. 413-422 (1990).

16. M. E. THOMPSON, "Numerical Simulation of Solute Transport in Rough Fractures," J. Geophys. Res., 96(B3), 4157 (1991).

17. G. ZYVOLOSKI, Z. DASH, and S. KELKAR, "FEHMN 1.0 Finite Element Heat and Mass Transfer Code," LA-12062-MS, Los Alamos National Laboratory (1991).

18. Y. W. TSANG, C. F. TSANG, I. NERETNIEKS, and L. MORENO, "Flow and Tracer Transport in Fractured Media: A Variable Aperture Channel Model and Its Properties," Water Resour. Res., 24(12), 2049 (1988).

19. Y. W. TSANG and C. F. TSANG, "Hydrological Characterization of Variable-Aperture Fractures," Rock Joints, Barton and Stephansson, eds., Balkema, Rotterdam, pp. 423-431 (1990).

20. P. PERSOFF, K. PRUESS, and L. MYER, "Two-Phase Flow Visualization and Relative Permeability Measurement in Transparent Replicas of Rough-Walled Rock Fractures," LBL-30161, Lawrence Berkeley Laboratory (1991).